Observation of the Coupling of Concentration Fluctuations to Steady-State Shear Flow

Noel A. Clark
Department of Physics, University of Colorado, Boulder, Colorado 80309

and

Bruce J. Ackerson
Department of Physics, Oklahoma State University, Stillwater, Oklahoma 74074

(Received 19 November 1979)

This Letter reports the first experimental study of the spatial structure of spontaneous thermal fluctuations for $ka \gtrsim 1$ in a physical system maintained in a nonequilibrium steady state. In particular, the shear-flow–induced distortion of the static structure factor, $S(\vec{k})$, is observed for a colloidal suspension of strongly interacting spherical particles of interparticle separation a.

PACS numbers: 61.90.+d

A wealth of information concerning the nonequilibrium behavior of fluids is available, in principle, in the evolution of their correlation functions and their spectral densities as the deviation from equilibrium is increased. This behavior has received some recent theoretical attention,[1-3] and has been observed via molecular dynamics.[4] It has not been reported in corresponding physical systems, since the basic condition for observability, namely that forced deviations from equilibrium be large enough to compete effectively with spontaneous fluctuations, often requires extreme experimental conditions. However, in systems with relatively slow fluctuations, such observations should be possible. Indeed, this coupling has recently been observed in the small-wave-vector ($\vec{k}$) and -frequency ($\Omega = 0$) limit for a binary mixture near the consolute point.[5]

In an equilibrium fluid of spherical particles the equal-time correlation function for particle concentration fluctuations, the position-dependent pair correlation function $g(\vec{r})$, and its spectral density, the static structure factor $S(\vec{k})$, are spherically symmetric in their respective spaces. A manifestation of this symmetry is the circular diffuse Debye-Scherrer ring(s) found in x-ray scattering studies of simple fluids. A steady-state shear flow applied to the fluid reduces this symmetry, distorting $g(\vec{r})$ and $S(\vec{k})$. This distortion is indirectly well known as it results in the major viscosity contribution in simple dense fluids.[6] This distortion has not been directly observed in noncritical atomic fluids since significant fractional changes in $S(\vec{k})$ require impractically high shear rates, S, comparable to the inverse of τ_a, the time characteristic of local rearrangement ($S \cong 10^{12}$ Hz).

In a macromolecular fluid, τ_a can be much longer. We consider a fluid of highly charged monodisperse polymer spheres in colloidal suspension. These suspensions have been shown to be quite useful as model systems of strongly interacting (repulsive) spherical particles, as the colloidal particles can assume solidlike, liquidlike, and gaslike structures.[7-9] The local rearrangement time for spheres in suspension is relatively long, being $\tau_a \sim a^2/D \sim 10^{-2}$ sec, where a is the intersphere separation and D the diffusion constant for the interacting spheres.

The coupling of a shear flow ($\vec{v} = \hat{z} S x$) to concentration fluctuations $[g(\vec{r})]$ may be expressed by writing the pair correlation function as a power series in $S \equiv \partial v_z/\partial x$. For S sufficiently small only the linear term need be kept and $g(\vec{r})$ is generally given by[10]

$$g(\vec{r}) = g_0(r)[1 + (xz/r^2)\nu(r)S], \tag{1}$$

where $g_0(r)$ is the equilibrium pair correlation function. The function $\nu(r)$ characterizes the radial dependence of the distortion of $g(\vec{r})$ induced by shear and must be calculated via a microscopic model. The simplest model is based on the Stokes assumption[4] that the viscous stress arising from the interactions of the spheres, ηS, is equivalent to the elastic stress $G\gamma$ where η is the viscosity, G is the local shear modulus, and γ is the strain of the fluid if the spheres could be sheared without flow. For this model the phenomenological local relaxation time is $\tau_a \equiv \eta/G$ and $g(\vec{r})$ has the form

$$g(\vec{r}) = g_0(r[1 - (xz/r^2)\tau_a S]) \tag{2}$$

or equivalently in the expansion presented in

Eq. (1),

$$\nu(r) = -\tau_a \frac{d \ln g_0(r)}{d \ln r} . \quad (3)$$

This Stokes model predicts, along lines of constant $\theta \equiv \tan^{-1}(x/z)$, a linear "stretch" of $g_0(r)$ of fractional magnitude $(\tau_a S \sin 2\theta)/2$. Fourier transformation shows a complementary elliptical distortion of the structure factor $S(\vec{k})$ for small rates of shear,

$$S(\vec{k}) = S_0(k[1 + \epsilon(k_x k_z/k^2)]), \quad (4)$$

where $\epsilon = \tau_a S$.

Alternatively, since $g_0(r)$ for deionized suspension of polymer spheres exhibits a strong nearest-neighbor peak at a radius a, we may consider a model in which a sphere is harmonically constrained to a spherical shell of radius a with a spring constant $\delta \equiv [d^2 U(r)/dr^2]_{r=a}$, where $U(r)$ is the effective interparticle potential $\{g_0(r) = \exp[-U(r)/k_B T]\}$. In the presence of the velocity field $\vec{v} = \hat{z} S x$, the diffusing sphere experiences an additional force $\vec{F} = \vec{v}/\mu$, where μ is the mobility. The resulting probability for finding the particle with respect to the origin can be found as a solution to the Smoluchowski equation[11] and is given by

$$g(\vec{r}) = N \exp\{-\beta[\delta(r-a)^2 - Sxz/\mu]/2\}, \quad (5)$$

where N is a normalization constant and S is assumed to be small. The form of Eq. (5) is not of the general form of Eq. (2) and displays a variation in the maximum amplitude of $g(\vec{r})$ as a function of θ, being largest at $\theta = 45°$ and 135°. However, the position of the maximum in $g(\vec{r})$ for a given θ is the position of null radial force. The positions of null radial force have the ellipsoidal symmetry of Eq. (2) with τ_a given by

$$\tau_a = 1/\delta\mu. \quad (6)$$

If we assume that $g_0(r)/g_0(a)$ reduces from unity at a to 0.5 at $0.8a$ and $1.2a$ in a quadratic fashion,[7] then from Eq. (6) we find that $\tau_a \cong 0.01$ sec for a water suspension of 0.1-μm-diam spheres at room temperature with $a = 1$ μm. This relaxation time is reasonable and results from a competition between the harmonic restoring force and the mobility, which is responsible for pushing the particle from equilibrium in the presence of a shear.

Two experimental geometries were employed to study $S(\vec{k})$ via light scattering in the presence of an applied shear. Here $\vec{k}$ is defined as the difference between the incident and scattered wave vectors, $\vec{k} = \vec{k}_I - \vec{k}_S$. One method uses a rocking cuvette as illustrated in Figs. 1(a) and 1(b). In this geometry $\vec{k}_I$ is normal to both v_z and $\hat{x}$, and $\vec{k}$ is nearly normal to $\vec{k}_I$. The cell is rocked about an axis parallel to $\vec{k}_I$ and normal to the largest cell face such that $\psi = \psi_0 \sin\omega t$. Because the fluid has inertia, the rocking induces the fluid motion indicated schematically in Fig. 1(b). This velocity relative to the cell is approximately of the form

$$\vec{V}(x,y,z) \cong -\hat{z}\omega\psi_0 x[1 - (2y/T_1)^2]\sin\omega t,$$

where T_1 is the width of the cell and the origin is at cell center. Typically $T_1 = 1$–2 mm, $0 < \omega < 20$ Hz, and $\psi_0 = \pi/8$ such that the Reynolds number of the flow is always less than 1% of the critical value for turbulence. Laser light of duration Δt $(\omega \Delta t \ll 1)$ is timed with the rocking cy-

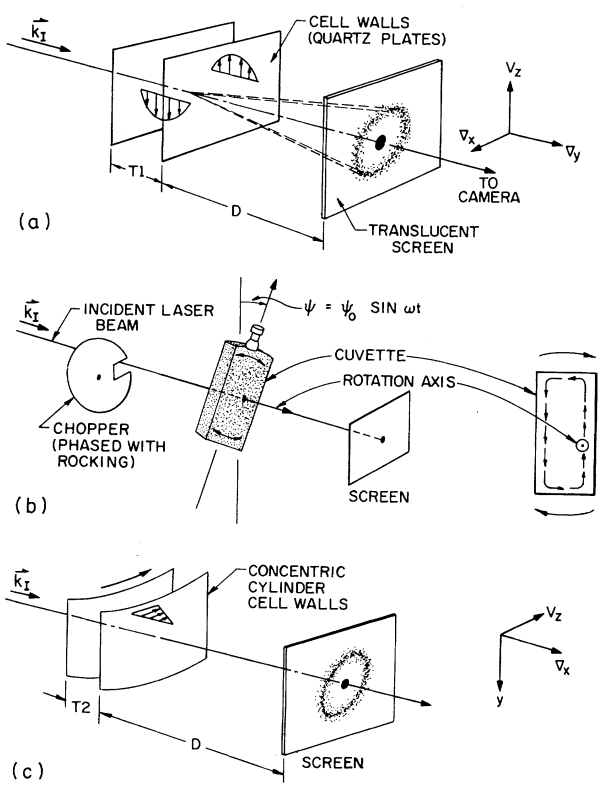

FIG. 1. (a), (b) The rocking-cuvette and (c) concentric-cylinder geometries. A shear is produced both perpendicular (∇_y) and parallel (∇_x) to the main face of the cuvette. The latter is responsible for the observed distortions of $S(\vec{k})$. The shear (∇_x) is perpendicular to the walls in the concentric cylinder method. The flow velocity is represented by v_z in both geometries. The widths of the cuvette and cylindrical cells are T_1 and T_2, respectively.

cle, such that $\dot{\psi}$ in the range $|\dot{\psi}| < \psi_0 \omega$ can be observed. The cell position can be adjusted so that the laser beam, which is collinear with the rocking axis, may pass through a selected region (x, z) of the cell. In this way, effects due to $\partial v_z/\partial y$ ($\propto x$) can be separated from those due to $\partial v_z/\partial x$, which is nearly constant versus x. The other experimental geometry employs a concentric quartz cylinder cell as shown in Fig. 1(c). The suspension is contained between the rotating inner cylinder wall (i.d. 29.0 mm) and outer cylinder wall (o.d. 36.5 mm). The incident wave vector, $\vec{k}_I$, is parallel to the shear, $\nabla\hat{x}$, and normal to the flow, v_z. While the induced shear is not perfectly linear because of the curvature of the cylindrical walls, it has the advantage that the velocity field is steady in time and not quasi-steady as in the rocking-cuvette method.

Samples were prepared using Dow polystyrene plastic spheres in which a small amount of H-OH ion-exchange resin in the cell bottom maintained the suspension in a highly deionized state. The quartz cuvette had dimensions $(1-2)\times 10\times 50$ mm^3 and contained either 0.109- or 0.234-μm-diam spheres at approximately 0.1 wt.% concentration. The concentric cylinder cell contained 0.109-μm-diam spheres at 0.16 wt.%.

Figure 2 shows intensity distributions obtained by scattering from suspensions in the cuvette. For $v_z = 0$, circularly symmetric Debye-Scherrer rings are seen [Figs. 2(b), 2(e)] while the ellipsoidal symmetry given by Eq. (4) is observed for nonzero shear [Figs. 2(a), 2(c), 2(d), 2(f)]. Control of S is achieved by varying either ω or the phase of the probe pulse during the rocking cycle. Figure 3 shows the variation of ϵ with S which we find to be linear over the range of S studied ($0 < S < 18$ Hz). Using Eq. (4) we find that the slope of ϵ vs S yields the effective relaxation times $\tau_a = 0.008 \pm 0.002$ sec ($d = 0.109$ μm) and $\tau_a = 0.013 \pm 0.003$ sec ($d = 0.234$ μm). The observed distortion of $S(\vec{k})$ with scattering from a similar sample in the concentric-cylinder geometry is much less pronounced than in the cuvette method because the incident wave vector is parallel to the shear. The Debye-Scherrer ring, which is circularly symmetric at zero shear, appears either to shift in a direction opposite to that of the flow velocity or to have just the leading edge in the $\hat{z}$ direction shifted slightly ($\Delta\theta \cong 1°$) in the $-\hat{z}$ direction. Relative intensity measurements were made of the leading edge to determine the shift or stretching of the first maximum in $S(\vec{k})$. The values of ϵ are determined from the peak shift via Eq. (4) and are shown in Fig. 3. The value of $\tau_a = 0.0084 \pm 0.001$ sec is determined from the slope of ϵ vs S at low shear. There is a broadening of the first maximum in $S(\vec{k})$ beyond that predicted by Eq. (4) as the rate of shear increases. This may be interpreted as a deviation of $U(r)$ from the approximation given in Eq. (3) and can be understood as a decrease in local or-

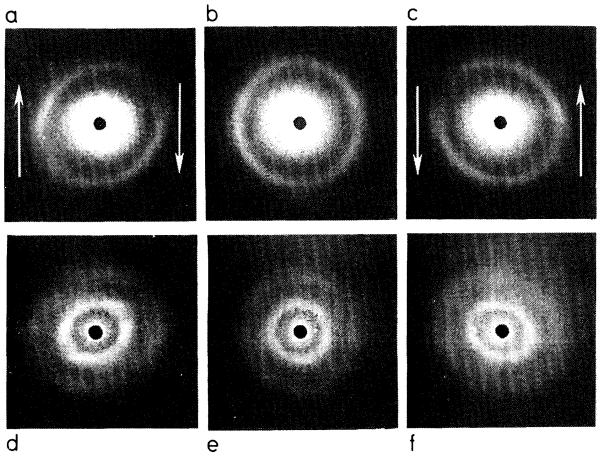

FIG. 2. Scattered-light intensity distributions obtained from colloidal suspensions of charged plastic spheres in a shear flow (indicated by white arrows) using the apparatus of Figs. 1(a) and 1(b). (a)–(c): 0.109-μm-diam spheres, $T_1 = 2$ mm, $D = 24.6$ mm [ring diameter on screen in (b) = 47 mm]. (a) $S = 2v_z/\partial x = -11.9$ Hz; (b) $S = 0$; (c) $S = +11.9$ Hz. (d)–(f): 0.234-μm-diam spheres, $T_1 = 1$ mm, $D = 47$ mm [ring diameter on screen in (e) = 21 mm]. (d) $S = -15.4$ Hz; (e) $S = 0$; (f) $S = 17.6$ Hz.

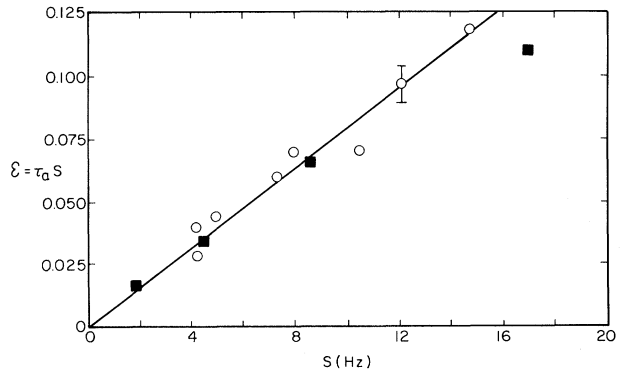

FIG. 3. The measured value of ϵ as a function of shear for 0.109-μm-diam spheres. Both data from the rocking cuvette (circles) and from the concentric-cylinder cell (squares) are presented. The line drawn through the data represents a relaxation time of 8.4 msec.

der due to the shear. The static structure factor is broadening and becoming more like that of a gas. In a gas the particles have a greater variation in separation. Measurements on the trailing edge ($k_y = 0$, $k_z < 0$) indicate similar results consistent with the general theoretical forms discussed.

Colloidal suspensions of highly charged particles have again[12,13] served as a model soft-sphere fluid and provided a means of studying model fluids, as well as real colloids. The position of the maximum intensity in $S(\vec{k})$ along lines of constant θ is given by a simple distortion model for the pair correlation function and can be used to measure the relaxation time τ_a. A harmonic model illustrates similar ellipsoidal symmetry with a variation in the maximum amplitude of $g(\vec{r})$ as a function of θ. A similar variation is noted in intensity on the Debye-Scherrer rings as a function of θ as seen in Fig. 2; however, a more sophisticated model is needed to explain these observations quantitatively.

This work was supported in part by a grant from the Research Corporation.

[1]I. Procaccia, D. Ronis, and I. Oppenheim, Phys. Rev. Lett. 42, 287, 614(E) (1979).
[2]J. Machta, I. Oppenheim, and I. Procaccia, Phys. Rev. Lett. 42, 1368 (1979).
[3]T. Kirkpatrick, E. D. G. Cohen, and J. R. Dorfman, Phys. Rev. Lett. 42, 862 (1979).
[4]W. T. Ashurst and W. G. Hoover, Phys. Rev. A 11, 658 (1975).
[5]D. Beysens, M. Gbadamassi, and L. Bouer, Phys. Rev. Lett. 43, 1253 (1979).
[6]H. S. Green, *The Molecular Theory of Fluids* (Dover, New York, 1969), p. 135ff.
[7]J. C. Brown, P. N. Pusey, J. W. Goodwin, and R. H. Ottewill, J. Phys. A 8, 664 (1975).
[8]D. W. Schaefer and B. J. Ackerson, Phys. Rev. Lett. 35, 1448 (1975).
[9]B. J. Ackerson, in *Photon Correlation Spectroscopy and Velocimetry*, edited by H. Z. Cummins and E. R. Pike (Plenum, New York, 1977), p. 344.
[10]J. A. Pryde, *The Liquid State* (Hutchinson, London, 1966), Chap. 9.
[11]C. A. Croxton, *Liquid State Physics* (Cambridge, London, 1974), p. 315 ff.
[12]P. A. Forsyth, S. Marcelja, D. J. Mitchell, and B. W. Ninham, Adv. Coll. Interface Sci. 9, 37 (1978).
[13]D. W. Schaefer, J. Chem. Phys. 66, 3980 (1977).

Evidence for Nonmonotonic Long-Range Interactions between Adsorbed Atoms

H.-W. Fink,[a] K. Faulian, and E. Bauer
Physikalisches Institut, Technische Universität Clausthal, D-3392 Clausthal-Zellerfeld, Federal Republic of Germany
(Received 3 December 1979)

The distribution function of the distance between a mobile and an immobile atom on a single-crystal surface has been measured for various temperatures, resulting in the first experimental demonstration of nonmonotonic long-range interactions. With W as the immobile atom and Pd as the mobile atom, at least two well-defined bond distances, 3.2 and 11 Å, are observed; with Re replacing W, at least one well-defined bond distance, 5.0 Å, and a strong anisotropy are seen. Additional bound states are indicated at larger distances.

PACS numbers: 68.20.+t, 73.20.Hb

The interaction between adsorbed atoms is one of the fundamental problems of surface physics. A considerable theoretical effort has been made, in particular during the past ten years, to obtain an understanding of these interactions (for a review, see Einstein[1]). Experiment, likewise, has been successful, for example, in measuring binding energies between dimers (for reviews, see Bassett and Tice,[2] Kellogg, Tsong, and Coulan,[3] Ehrlich,[4] and Tsong and Cowan[5]). The experimental confirmation of one of the major predictions of the theory, that of long-range oscillatory interactions, however, has been elusive. An apparently successful attempt at such a confirmation by field-ion microscopy (FIM), with Re atoms on a W(110) surface,[6] was later shown to be inconclusive for Re on W(110),[2] W(112), and W(123) (Ref. 7) surfaces. The only well-founded results indicating an "abnormal" distance dependence of the adatom interactions are limited to short distances: The (internal) binding energy of a Re dimer on W(112) with the smallest adatom distance (4.48 Å) is smaller than that with the next largest distance (5.25 Å) (100 ± 50 vs 165 ± 50

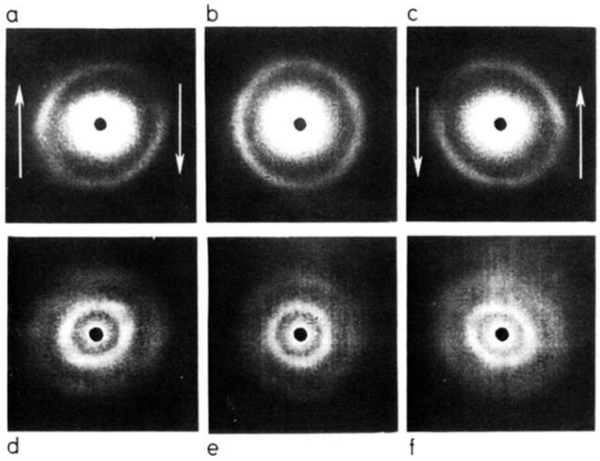

FIG. 2. Scattered-light intensity distributions obtained from colloidal suspensions of charged plastic spheres in a shear flow (indicated by white arrows) using the apparatus of Figs. 1(a) and 1(b). (a)–(c): 0.109-μm-diam spheres, $T_1 = 2$ mm, $D = 24.6$ mm [ring diameter on screen in (b) = 47 mm]. (a) $S = 2v_z/\partial x = -11.9$ Hz; (b) $S = 0$; (c) $S = +11.9$ Hz. (d)–(f): 0.234-μm-diam spheres, $T_1 = 1$ mm, $D = 47$ mm [ring diameter on screen in (e) = 21 mm]. (d) $S = -15.4$ Hz; (e) $S = 0$; (f) $S = 17.6$ Hz.